01 Dec 2006

Differential Electron Emission for Single and Multiple Ionization of Argon by 500 EV Positrons

Jared M. Gavin

Robert D. DuBois
Missouri University of Science and Technology, dubois@mst.edu

O. G. de Lucio

Recommended Citation

J. M. Gavin et al., "Differential Electron Emission for Single and Multiple Ionization of Argon by 500 EV Positrons," *Physical Review Letters*, American Physical Society (APS), Dec 2006.
The definitive version is available at https://doi.org/10.1103/PhysRevLett.97.243201

Differential Electron Emission for Single and Multiple Ionization of Argon by 500 eV Positrons

O. G. de Lucio, J. Gavin, and R. D. DuBois

Department of Physics, University of Missouri-Rolla, Rolla, Missouri 65409 USA

(Received 29 August 2006; published 14 December 2006)

Triply differential electron emission cross sections are measured for single ionization of argon by 500 eV positrons. Data are presented for coincidences between projectiles scattered into angles of 3° and electrons with emission energies less than 10 eV that are observed between 45 and 135° along the beam direction. For interpretation, these are compared to cosine squared representations of the binary and recoil lobes which are convoluted over experimental parameters. Singly differential electron emission data for double and triple ionization by positrons are also presented.

DOI: 10.1103/PhysRevLett.97.243201 PACS numbers: 34.50.Fa, 34.50.Bw, 34.80.Dp, 34.85.+x

Introduction.—For decades, a major goal of atomic physics research has been to understand and model the time evolution of interactions between atomic particles. Energy and momentum transfer during these interactions result in bound electrons being excited, ionized, or transferred from one particle to the other. In addition, molecular fragmentation can occur, and electrons, ions, and atoms can be ejected from the surface during interactions with solids. Thus understanding atomic interactions and dynamics plays a key role in diverse areas such as improved lighting sources, chemical reactions, atmospheric and interstellar physics, radiation damage to solids and biological tissue, and plasma processes.

Although the Coulomb force between two isolated charges can be calculated exactly, any interaction involving even the simplest atom or molecule must model the time evolution of many, mutually coupled forces; this can only be done using various approximations. As a further complication, even for interactions where the coulomb forces have the same magnitude, the masses of the particles influence the amount of energy and momentum that can be transferred and the sign of the charge influences such things as exchange processes, polarization effects, and post-collision effects. For many decades experimental data for positron, electron, and proton impact have been compared in order to provide insight into these effects and to test theoretical models and provide a deeper understanding of the interactions and dynamics. For example, comparing positron and electron impact has shown that at high velocities the total cross sections for single target ionization are nearly identical, whereas the double ionization cross sections for electron impact are roughly a factor of 2 larger [1]. Recent studies [2] also imply that for single ionization of heavier atoms there may be differences between electron and proton impact. Simple, one-electron perturbation theories cannot account for these effects; more sophisticated theoretical treatments are required.

Fully differential experimental data, traditionally referred to as triply differential cross sections (TDCS), have provided the most sensitive tests of theory to date. For electron impact fully differential data have been available since the pioneering studies of Ehrhardt and coworkers [3]. For ion and photon impact, the development of the recoil ion momentum spectroscopy method (See Ref. [4] and references therein) has yielded fully differential data for single as well as for multiple target ionization. Unfortunately, because of the much weaker beam intensities available, very little differential ionization data is available for positron impact. Singly differential data has been reported by Falke *et al.* [5] while Schmitt *et al.* [6] and Kövér and Laricchia and coworkers [7,8] have performed several doubly differential electron emission studies. In our laboratory we have measured doubly differential energy loss yields for scattered positrons [9,10]. The only TDCS data for positron impact are from experiments designed to investigate electron capture to the continuum [11–13] where the data are limited to scattered positrons and ejected electrons both being observed at zero degrees. As such, these data provide only limited tests of theory and no direct comparison to available electron or proton impact data can be made.

To help answer these questions, we report here TDCS data for single ionization of argon induced by 500 eV positron impact. In addition, we present the first experimental information for differential electron emission resulting from multiple ionization in antiparticle-particle interactions, namely, singly differential electron emission data for double and triple ionization of argon by positrons.

Experimental method and data analysis.—Much of the experimental apparatus shown in Fig. 1 has been described previously [9,10]. Briefly, a ^{22}Na radioactive source and tungsten moderator followed by an electrostatic beam transport system inject a 6 mm diameter positron beam into the target chamber where it crosses a gas jet. Target ions are extracted by a 2 V/cm electric field while forward scattered positrons are energy analyzed by an electrostatic analyzer and detected by a position-sensitive channelplate detector (PSD). Modifications for our present study include using a 6 mm aperture and a channel electron multiplier to detect target ions originating from the beam-gas jet overlap

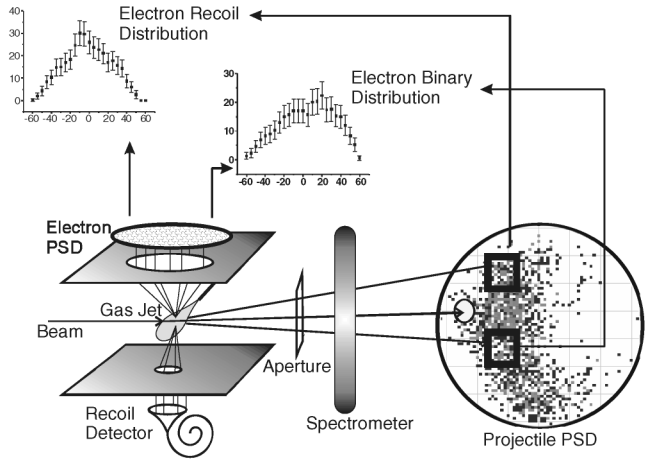

FIG. 1. Schematic view of experimental apparatus. The insets show electron emission and positron scattering and energy loss for single ionization.

region and installing a 50 mm diameter two-dimensional PSD opposite the recoil ion detector to detect electrons. In the absence of any electric fields, this detector is sensitive to electron emission angles of $45° < \theta_e < 135°$ along the beam direction and $\varphi_e < \pm 45°$ perpendicular to a scattering plane which is defined by the entrance slit to the projectile energy analyzer. For our setup, the electric field used to extract target ions allows low-energy electrons ejected into angles outside these ranges to also be detected.

Positrons, scattered into horizontal angles φ_p of $0° \pm 2.4°$ and vertical angles θ_p of $0° \pm 7.5°$, pass through a vertical slit and enter the electrostatic energy spectrometer which focuses different φ_p angles onto the projectile PSD. There is no focusing in the vertical direction so θ_p scattering angle information is preserved. For the present experiment, we detected positrons with energies between ~500 and 420 eV. Because of our positron beam diameter, our detected energy and angular resolutions were measured to be Gaussian with half widths of approximately ± 5 eV and $\pm 1°$. These are taken into account in determining the energy loss and scattering angles for our TDCS measurements. The positron beam intensity was approximately 2000 particles/sec, the electron intensity roughly an order of magnitude smaller, and the recoil ion rate was less than 1 particle/sec. This provided a triple coincidence signal of approximately one count every 15 minutes. The data presented here were accumulated over a period of two months.

For data collection, the spectrometer voltages were adjusted to detect the primary beam plus a range of energy losses and scattering angles. Using recoil ions as an event trigger, target ion-ejected electron and target ion-scattered positron coincidences were measured in list-mode using standard electronics, time to digital converters and a PC. Sorting these data using various combinations of windows set on the time-of-flight spectra and/or on the electron or positron detection positions, information about (a) the electron emission as a function of angle, θ_e and φ_e; (b) the positron energy loss, ΔE, and scattering angle, θ_p; and (c) correlations between ejected electrons and scattered positrons, i.e., TDCS, were obtained for single and for multiple ionizing interactions. Background contributions were also determined.

The 2D projectile spectrum in Fig. 1 illustrates one example of what is learned by this approach. Here scattered positron-ejected electron-singly charged recoil ion coincidences illustrate the well-known correlation between projectile energy loss and scattering angle for single ionization. The maximum intensity occurring along a "binary ridge" is clearly seen. However, an "up-down" asymmetry for larger energy losses is also apparent. This asymmetry is because the electron detector is sensitive to electrons being ejected in the "up" direction which means that for higher energy losses where binary interactions dominate, the positron is scattered "down". These down scattered projectiles primarily correlate with forward electron emission, i.e., the binary lobe. The coincidence signal seen for up scattered positrons means that the electron and positron left the interaction region in the same hemisphere. This indicates that a third body is involved; i.e., recoil events are occurring. These up scattered projectiles primarily correlate with backward electron emission, e.g., the recoil lobe. Thus, the positron 2D coincidence spectrum directly illustrates the relative importance of binary versus recoil interactions as a function of energy loss. As seen, the probabilities are roughly equivalent for small energy loss whereas binary interactions become more important with increasing energy loss. Note that these data are for all observed electron emission angles; i.e., they represent triply differential cross sections integrated over a range of electron angles.

Another example is illustrated by the two 1D spectra in Fig. 1 showing the electron emission angle dependence associated with up and down scattered positrons, i.e., the angular dependences for recoil and binary interactions. For binary collisions the primary electron emission is in the forward direction while recoil interactions generate more emission in the backward direction and at larger angles. Again these data are for single ionization events. They illustrate the cumulative emission for many electron energies. However, as will be discussed below, the electric field used to extract target ions strongly influences these spectra.

By combining the positron and electron information we can obtain fully differential kinematic information for single ionization. Our method was to select electron data associated with a specific range of positron energy losses and for symmetric up-down scattering angles, as indicated by the boxes in the projectile PSD spectrum in Fig. 1. For the positron, the boxes plus entrance slit define the positron energy and both scattering angles, while for the electron the emission angles are extracted from the detected position and the energy is determined from the projectile

energy loss. Thus all parameters are known. As our extended beam image and finite box size lead to a range of energy losses, in presenting our data we define two quantities, namely, the Gaussian centroid energy for the energy loss range selected and the mean energy of all electrons contributing to the measured cross sections. Finally, to improve statistics we have summed our 2D fully differential electron emission data over a range of $\pm\varphi_e$ angles and binned the data along the beam direction.

Results and discussion.—Figure 2 presents two examples of our positron impact fully differential data for single ionization of argon by 500 eV positrons. The mean electron energies are 2.4 and 7.3 eV, and the projectile scattering angle range is 1.5° to 4.5°. Centroid energies are also listed. We present the data in the traditional manner using polar plots but the reader should note that the angles plotted are not the initial directions that the electrons are emitted; rather they are the geometric angles calculated using the detection position and a point at the center of the beam-gas jet overlap. This means that influences on the electron trajectories by the recoil ion extraction field are not taken into account; i.e., for low electron energies, the geometric and initial emission angles can be quite different.

At first glance, these data indicate the expected binary and recoil lobes for electron emission, the upward and downward lobes, respectively. In addition, for lower energy electron emission the lobes are broader and demonstrate structure. One also notes that if two-body kinematics and the mean electron energy combined with beam diameter and positron scattering angle box size information are used to calculate the direction (radial arrows) and range (double headed arrows) of expected momentum transfer, our observed lobes are shifted to larger angles.

To understand these features and to investigate the influence of various experimental parameters on the data, a computer program was written where all geometric properties and electric fields were included. Cosine squared functions where the relative intensities and directions were left as free parameters were used to simulate the binary and recoil electron emission probabilities. These were convoluted over emission energy, positron scattering angle, scattering plane, interaction volume, etc. To best reproduce our experimental data, we found that the relative recoil to binary intensities needed to be approximately equal at 1 eV and slowly decrease to 1/3 at 20 eV. In addition, to match the 2.4 eV data it was necessary to shift the positions of the binary and recoil peaks to smaller angles by 10° and 40°, whereas to match the 7.3 eV data a 10° shift to larger angles was required. Values intermediate to these were found for energies between 2.4 and 7.3 eV.

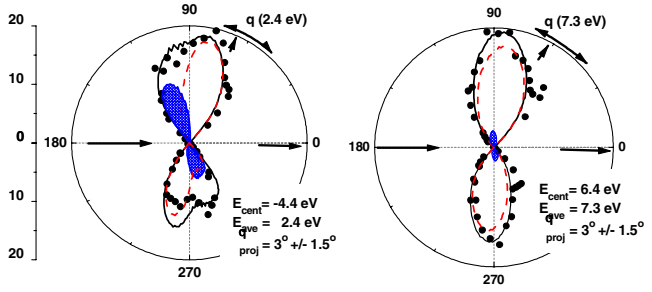

FIG. 2 (color online). Triply differential electron emission yields for single ionization of argon by 500 eV positrons. Experimental data: "horizontal" arrows represent the initial and scattered positron directions; radial and curved arrows show momentum transfer direction and range. The solid and dashed lines and the filled areas are simulated curves for the binary and recoil emission convoluted over experimental conditions.

The convolutions are shown in Fig. 2 by the solid curves. These curves are the sum of "real" binary and recoil electrons, indicated by the larger dashed lobes centered at angles smaller than 90° and 270°, and "false" electrons, indicated by the smaller filled lobes at angles larger than 90° and 270°. The false curves represent low-energy binary and recoil electrons which are initially emitted away from the electron detector but are turned around by the electric field. As seen, when the mean electron energy is small, the contribution of false electrons is large and asymmetric or double lobed features appear. For larger energies, very few electrons are turned around and the false lobes are small. Our simulations also demonstrated that the observed maxima and widths of the lobes are altered due to decreases in grid transmission with increasing angle of incidence plus detection solid angle and electric field effects. These lead to increasing truncation of the observed electron intensities at forward and backward angles, i.e., altered peak width and direction.

Finally, our present study also goes beyond single ionization and provides the first experimental differential data for electron emission resulting from multiple ionization by an antiparticle. By integrating our two-dimensional ejected electron-target ion coincidence spectra over a narrow φ_e range, singly differential yields, $d\sigma/d\theta_e$, for single, double, and triple ionization were obtained as a function of θ_e. Ratios of these values are shown in Fig. 3. As seen, double and triple ionization contribute approximately 10% and 2% to the total angular dependence. With respect to interaction dynamics, the percentage of multiple ionization increases for backward electron emission and this percentage increases with degree of ionization. This is consistent with backward electron emission requiring a subsequent interaction between the outgoing electron and a third body; since multiple ionization inherently involves many bodies it should result in enhanced backward emission.

In conclusion, fully kinematical data for single ionization by positrons and the very first experimental information relating to differential multiple electron emission resulting from antiparticle impact have been presented. The data and methods outlined here provide the basis for

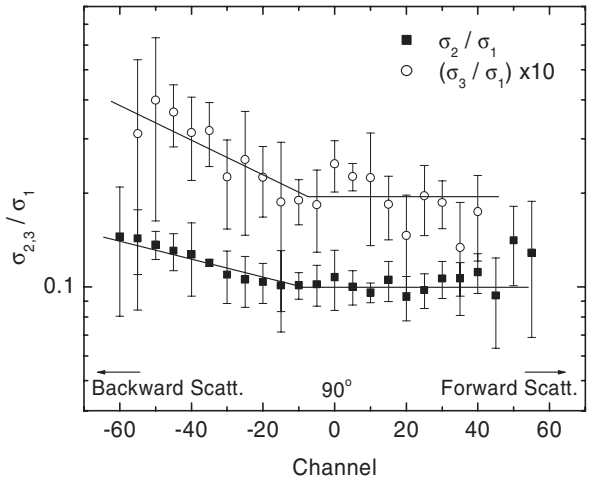

FIG. 3. Ratios of singly differential electron emission cross sections, $\sigma(\theta_e)$, resulting from multiple versus single ionization of argon by 500 eV positrons.

testing our understanding of collision dynamics in unprecedented detail and achieve a decades old goal, namely, TDCS information for antiparticle-particle interactions. Our next studies will concentrate on improving our energy resolution, investigating a broader range of energy losses, scattering and electron emission angles, and better defining a collision plane, plus decreasing the influence of the electric field. In addition, in the near future we plan to install an electron gun in order to investigate and compare positron and electron impact data under identical experimental conditions, the goal being to probe charge dependent kinematical effects in unprecedented detail.

This work was supported by the National Science Foundation.

[1] H. Bluhme *et al.*, J. Phys. B **32**, 5835 (1999), and references therein.
[2] E. G. Cavalcanti *et al.*, J. Phys. B **36**, 3087 (2003).
[3] H. Ehrhardt *et al.*, Phys. Rev. Lett. **22**, 89 (1969).
[4] *Many-particle quantum dynamics in atomic and molecular fragmentation*, edited by J. Ullrich and V. P. Shevelko, in Springer series on "Atomic, Optical and Plasma Physics" (Springer-Verlag, Berlin, 2003), pp 37 and 253.
[5] T. Falke *et al.*, J. Phys. B **30**, 3247 (1997).
[6] A. Schmitt *et al.*, Phys. Rev. A **49**, R5 (1994).
[7] Á. Kövér *et al.*, J. Phys. B **30**, L507 (1997) and references therein.
[8] Á. Kövér, G. Laricchia, and M. Charlton, J. Phys. B **27**, 2409 (1994) and references therein.
[9] R. D. DuBois *et al.*, J. Phys. B **34**, L783 (2001).
[10] A. C. F. Santos, A. Hasan, and R. D. DuBois, Phys. Rev. A **69**, 032706 (2004).
[11] Á. Kövérand and G. Laricchia, Phys. Rev. Lett. **80**, 5309 (1998).
[12] Á. Kövér, K. Paludan, and G. Laricchia, J. Phys. B **34**, L219 (2001).
[13] Á. Kövér, G. Laricchia, and M. Charlton, J. Phys. B **26**, L575 (1993).